International Research Journal on Advanced Engineering and Management
https://goldncloudpublications.com
https://doi.org/10.47392/IRJAEM.2026.0410
e ISSN: 2584-2854
Volume: 04 Issue: 10
October 2026
Page No: 2910 - 2916

Raman Spectroscopic Study of Solid-State and Sol–Gel $ZnWO_4$ and the Effect of Eu^{3+} Doping Concentration on Vibrational Properties

Vinod Kumar[1], Dr. Rakesh Kumar[2]
[1]Assistant Professor, Department of Physics, Government Degree College, Agra Cantt, Agra 282001
[2]Assistant professor, Department of Physics, Narain College Shikohabad, District-Firozabad (U.P.) 283135
Emails: *vinodtyagi1972@gmail.com[1], dr.rkyadavndc@gmail.com[2]*

Abstract
The Raman spectra of pure $ZnWO_4$ prepared by solid-state and sol–gel methods and of solid-state $ZnWO_4$ doped with 1% and 2% Eu^{3+} were investigated. All samples showed the characteristic monoclinic wolframite spectrum, dominated by the symmetric W–O stretching band near 907 cm^{-1}. The 1% and 2% Eu^{3+} samples, measured under identical conditions, gave practically identical spectra, with band positions agreeing within 0.1–0.3 cm^{-1}, equal linewidths and no new bands, so no Eu^{3+}-dependent change of the WO_6 framework was detected. The uniform downshift of about 1 cm^{-1} of all bands relative to the pure solid-state sample was attributed to the different excitation wavelength and grating, not to doping. The sol–gel sample showed slightly lower band positions, broader low-frequency bands, a strong fluorescent background and a weak band near 926 cm^{-1}, indicating somewhat lower structural order.

Keywords: *Raman Spectroscopy; Eu^{3+} Doping; Sol–Gel Synthesis; Solid-State Synthesis*

1. Introduction
Zinc tungstate ($ZnWO_4$) is an important inorganic functional material that has attracted considerable attention because of its distinctive crystal structure, excellent chemical stability, and potential applications in scintillation detectors, photonic devices, and luminescent materials [1], [2]. $ZnWO_4$ crystallizes in a monoclinic wolframite structure in which the local coordination of Zn^{2+} and W^{6+} ions contributes to its characteristic vibrational behavior. Raman spectroscopy is a valuable technique for investigating these vibrational properties because it provides information about lattice vibrations, metal–oxygen bonding, and structural changes within the crystal [3], [4]. The synthesis route can influence crystallinity, particle morphology and local structural order. Therefore a comparison between solid-state and sol-gel synthesized $ZnWO_4$ is particularly relevant. Solid-state synthesis is generally performed through the reaction of precursor powders at high temperatures. The sol–gel method provides molecular-level mixing and the possibility of enhanced compositional homogeneity [5], [6]. Another way to alter the structural and vibrational properties of $ZnWO_4$ is doping with rare earth elements. Europium (Eu^{3+}) is of special interest because its incorporation can influence the local coordination environment, lattice distortion and bonding interactions. However, the effects may depend on the doping concentration and charge-compensation mechanisms involved in substitution of Eu^{3+} for Zn^{2+} [7], [8]. Thus, Raman analysis of undoped and Eu^{3+} -doped $ZnWO_4$ prepared by different synthesis routes can help to clarify the differences in the vibrational modes and their relation with the material structure [9]. The present study deals with the Raman spectroscopic properties of solid-state and sol–gel synthesised $ZnWO_4$ and the effect of Eu^{3+} doping

International Research Journal on Advanced Engineering and Management
https://goldncloudpublications.com
https://doi.org/10.47392/IRJAEM.2026.0410
e ISSN: 2584-2854
Volume: 04 Issue: 10
October 2026
Page No: 2910 - 2916

concentration on its vibrational properties. The comparison aims to improve the understanding of the synthesis-dependent and concentration-dependent changes of the vibrational behaviour of $ZnWO_4$ phosphors.

1.1.Zinc Tungstate ($ZnWO_4$): Crystal Structure and Material Characteristics

$ZnWO_4$ crystallizes in the monoclinic wolframite structure, space group P2/c, with two formula units in the cell. Both metal ions sit in distorted octahedra of oxygen. Zinc occupies ZnO_6 units, and tungsten occupies WO_6 units, and the octahedra share edges to form zigzag chains that run through the crystal [10]. Each tungsten ion has a few short W–O bonds and a few longer ones, and it is this distortion that gives the lattice its characteristic vibrations. The compound has been studied for its luminescence, its scintillation behaviour and its photocatalytic activity, and its stability in air makes it convenient to handle [11]. It is commonly prepared by solid-state reaction, where oxide precursors are ground together and heated at high temperature, which usually gives well-crystallized powders with fairly large particles. Wet-chemical methods such as sol–gel synthesis start from solutions and generally yield finer powders at lower processing temperatures, but they can leave more defects or residual species. Since the same compound can therefore differ in crystallinity and defect content depending on how it is made, the synthesis route is an important variable and has to be considered when properties are compared [12].

1.2.Europium (Eu^{3+}) Doping and Its Influence on $ZnWO_4$

Europium is widely used as an activator in tungstate hosts, because Eu^{3+} gives sharp red emission. For the dopant to work, however, it has to be accommodated in the lattice, and $ZnWO_4$ does not make this easy. In sixfold coordination Eu^{3+} has an ionic radius of about 0.95 Å, noticeably larger than Zn^{2+} at about 0.74 Å, and it carries a different charge [13]. If Eu^{3+} replaces Zn^{2+}, the lattice must compensate for the extra positive charge, most simply through zinc vacancies or other defects. The surrounding ZnO_6 octahedra may expand, and the neighbouring WO_6 units may be pushed slightly out of shape [14]. These effects should grow with the amount of europium added, although not necessarily in a straight line. At higher concentrations the dopant may also separate as a second phase instead of entering the lattice. The Eu^{3+} content therefore needs to be examined carefully, and low concentrations such as 1% and 2% are particularly useful, because they show whether small additions already leave a mark on the host. Whether a given change comes from real incorporation of the dopant or from some other cause has to be checked by experiment, and cannot be assumed [15][16].

1.3.Significance of Vibrational Properties in $ZnWO_4$ Phosphors

Raman spectroscopy probes the vibrations of a crystal, and for $ZnWO_4$ it is especially informative. Factor-group analysis of the wolframite structure predicts eighteen Raman-active modes, eight of Ag symmetry and ten of Bg symmetry. The strongest band appears near 907 cm^{-1} and comes from the symmetric stretching of the short W–O bonds in the WO_6 octahedra [17] [1]. Weaker bands at lower wavenumbers arise from other W–O stretches, from vibrations of the W–O–W bridges, and from bending and lattice motions that involve the zinc ions. Because each band belongs to a particular type of motion, a shift in position suggests a change in bond strength, a change in width points to disorder or defects, and a new band may indicate another phase [18]. These features are useful for Eu^{3+}-doped samples, where the dopant is expected to disturb the local bonding only slightly. Raman results must be read with care, though, since band positions and widths also depend on the excitation wavelength, the grating and the laser power. Measurement conditions therefore have to be recorded and compared before any shift is assigned to doping [19].

2. Research Gap and Motivation

Zinc tungstate $ZnWO_4$ is a wolframite-type host whose Raman spectrum is strongly sensitive to the W-O bonding of the WO_6 octahedra, and to the

International Research Journal on Advanced Engineering and Management
https://goldncloudpublications.com
https://doi.org/10.47392/IRJAEM.2026.0410
e ISSN: 2584-2854
Volume: 04 Issue: 10
October 2026
Page No: 2910 - 2916

degree of order of the lattice. Eu^{3+} is larger than Zn^{2+} and incorporation may therefore distort the local environment. But it is not yet known if low concentrations of Eu^{3+} can lead to observable changes in the Raman bands. In addition, ZnWO4 can be prepared by solid state and sol–gel methods that differ in crystallite size and defect concentration, but their vibrational spectra have rarely been compared to those of Eu^{3+} -doped samples. The Raman band positions and widths also depend on the excitation wavelength, grating and laser power, which adds to the complexity of interpretation. Doping effects need to be distinguished from measurement effects. Therefore, the present study investigates pure $ZnWO_4$ prepared by solid-state and sol-gel methods and solid-state $ZnWO_4$ doped with 1% and 2% Eu3+ using only Raman spectroscopy. It separates the effects of composition, synthesis route and measurement configuration.

3. Objectives And Novelty of the Present Study

The main objectives of this study are:

1. To prepare pure $ZnWO_4$ by the solid-state and sol–gel methods, and Eu^{3+}-doped $ZnWO_4$ (1% and 2%) by the solid-state method.
2. To identify the Raman-active modes of the wolframite structure and their assignment to W–O and Zn–O vibrations in all samples.
3. To determine whether increasing the Eu^{3+} concentration from 1% to 2% changes the position, width or number of Raman bands.
4. To compare the Raman spectra of solid-state and sol–gel $ZnWO_4$ in terms of band position, linewidth, background and structural order.
5. To separate genuine composition and synthesis effects from differences caused by the measurement configuration.

4. Material And Methods

4.1.Synthesis of $ZnWO_4$ and Eu^{3+}-doped $ZnWO_4$

Pure $ZnWO_4$ was prepared by a conventional solid-state method and a citrate sol–gel method, while Eu^{3+}-doped $ZnWO_4$ (nominal 1% and 2%) was prepared by the solid-state method only. The four samples are denoted ZWO-SS, ZWO-SG, SS:1Eu and SS:2Eu.

Route A: $ZnWO_4$ was used as the host precursor, with Eu_2O_3 as the europium source for the doped samples. The precursors were weighed in stoichiometric ratios and ground in an agate mortar and pestle for 2 h, using acetone as the homogenizing medium. The dried powders were placed in alumina crucibles and heated in a muffle furnace at 900 °C for 5 h in air, then cooled naturally to room temperature inside the furnace.

Route B: Stoichiometric amounts of $Zn(NO_3)_2{\cdot}6H_2O$ and $Na_2WO_4{\cdot}2H_2O$ were each dissolved separately in deionized water. The $Na_2WO_4{\cdot}2H_2O$ solution was added dropwise to the $Zn(NO_3)_2{\cdot}6H_2O$ solution, and citric acid was added as a chelating agent (metal ion to citric acid ratio of 1:1). The mixture was stirred continuously at 80 °C until the solvent evaporated and a viscous, transparent gel formed. The gel was dried and calcined at 450 °C for 3 h to obtain pure $ZnWO_4$.

4.2.Raman spectroscopy

Raman spectra were recorded with a Renishaw Raman spectrometer with ×50 objective and Renishaw Centrus detector, controlled by WiRE software. Each spectrum is a single scan, 10 s long, with one accumulation from 101.6 to 1002.4 cm^{-1} at a spectral sampling interval of approximately 1.2 to 1.3 cm^{-1}. The excitation wavelength, laser power, grating and focus mode for each samples are shown in Table 1. The sol-gel sample and the doped samples were measured using a 532 nm laser and a 2400 lines/mm grating and the pure solid-state sample was measured using a 785 nm laser and a 1200 lines/mm grating.

Table 1 Raman acquisition conditions for the samples studied

Sample	Synthesis route	Laser (nm)	Power (%)	Grating (lines/mm)	Focus mode

International Research Journal on Advanced Engineering and Management
https://goldncloudpublications.com
https://doi.org/10.47392/IRJAEM.2026.0410
e ISSN: 2584-2854
Volume: 04 Issue: 10
October 2026
Page No: 2910 - 2916

ZWO-SS	Solid-state	785	0.05	1200	Line
ZWO-SG	Citrate sol–gel	532	5	2400	Regular
SS:1Eu	Solid-state, 1% Eu^{3+}	532	1	2400	Regular
SS:2Eu	Solid-state, 2% Eu^{3+}	532	1	2400	Regular

All spectra: ×50 objective, 10 s exposure, one accumulation, continuous scan, 101.6–1002.4 cm^{-1}.

4.3.Data analysis

For display and normalization, a smooth baseline was subtracted. Band positions and full widths at half maximum (FWHM) were obtained by fitting each band with a Lorentzian function and a local linear background. The same procedure was applied to all four spectra. Typical fit uncertainties in band position were 0.1-0.3 cm-1 and 1-3 cm-1 for the weak, broad bands of the sol-gel sample. The absolute calibration is limited by the spectral sampling interval of 1.2 to 1.3 cm^{-1}.

5. Result And Discussion

5.1.Raman spectra and band assignment

The Raman spectra of pure $ZnWO_4$ prepared by the solid-state method (ZWO-SS) and the sol–gel method (ZWO-SG), and of solid-state $ZnWO_4$ with 1% and 2% Eu^{3+} (SS:1Eu and SS:2Eu), are compared in Fig. 1. All samples show the characteristic spectrum of monoclinic wolframite $ZnWO_4$ (P2/c; 8Ag + 10Bg Raman-active modes), with a dominant band at about 907 cm^{-1} and weaker bands at about 123, 164, 194, 275, 314, 342, 408, 546, 678, 709 and 787 cm^{-1} (Table 2). The 907 cm^{-1} band is the symmetric Ag stretching mode of the short W–O bonds of the WO_6 octahedra. The bands at 678–787 cm^{-1} are other W–O stretching modes, and the 546 cm^{-1} band arises from W–O–W bridge vibrations. The bands at 300–410 cm^{-1} are attributed to W–O bending and Zn–O vibrations, and those below 280 cm^{-1} to external lattice modes. Both synthesis routes therefore give the wolframite phase, and it is retained at 1% and 2% Eu^{3+}. As shown in Figure 1 (a) Raman spectra of ZWO-SS (785 nm), ZWO-SG (532 nm), SS:1Eu and SS:2Eu (532 nm) after baseline subtraction and normalisation to the strongest band; curves are offset. (b) Expanded view of the band near 907 cm^{-1}, As shown in Table 2 Raman band positions (cm^{-1}) and the FWHM of the main band.

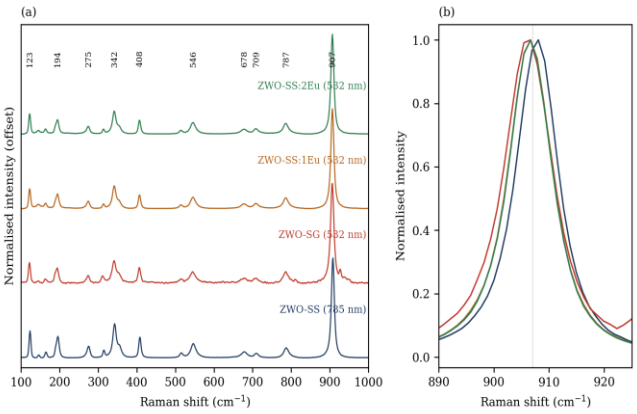


Figure 1 (a) Raman spectra of ZWO-SS (785 nm), ZWO-SG (532 nm), SS:1Eu and SS:2Eu (532 nm) after baseline subtraction and normalisation to the strongest band; curves are offset. (b) Expanded view of the band near 907 cm^{-1}

Table 2 Raman band positions (cm^{-1}) and the FWHM of the main band

Band	ZWO-SS (785 nm)	ZWO-SG (532 nm)	1% Eu (532 nm)	2% Eu (532 nm)
Lattice	123.3	121.8	122.4	122.4
Lattice	194.9	192.9	194.0	193.8
Bending	342.3	340.8	341.3	341.3
Bending	407.9	406.5	406.9	406.9
W–O–W bridge	546.3	544.6	545.3	545.2
W–O stretch (Bg)	787.0	785.5	785.8	785.7
W–O stretch	907.8	906.2	906.6	906.6

International Research Journal on Advanced Engineering and Management
https://goldncloudpublications.com
https://doi.org/10.47392/IRJAEM.2026.0410
e ISSN: 2584-2854
Volume: 04 Issue: 10
October 2026
Page No: 2910 - 2916

(Ag)				
FWHM of main band	9.0	10.0	9.4	9.3

Positions from Lorentzian fits with a local linear background; fit uncertainty typically 0.1–0.3 cm^{-1}, spectral sampling interval ≈ 1.2–1.3 cm^{-1}.

5.2.Effect of Eu^{3+} concentration

The spectra of the 1% and 2% Eu^{3+} samples, measured under identical conditions, are practically identical. The bands coincide within 0.1–0.3 cm^{-1} (main band at 906.6 cm^{-1} in both), the linewidths are equal (Fig. 2b), and no new bands appear. Increasing the Eu^{3+} content from 1% to 2% therefore produces no detectable change in the WO_6 framework. Relative to ZWO-SS, all bands of the doped samples lie lower by a nearly constant 1.0 ± 0.2 cm^{-1} (Fig. 2a). The shift is the same at every wavenumber and for both concentrations, which points to the different excitation (785 vs 532 nm) and grating (1200 vs 2400 lines/mm), not to a dopant effect.

5.3.Solid-state versus sol–gel $ZnWO_4$

ZWO-SG was measured with the same laser, grating and focus as the doped samples (laser power 5% versus 1%). Its spectrum contains the same set of wolframite bands, showing that the sol–gel product is crystalline $ZnWO_4$. Compared with the solid-state samples, however, its bands are 0.3–1.0 cm^{-1} lower, most clearly for the lattice and bending modes, and they are broader (Fig. 2). The main band has a FWHM of 10.0 cm^{-1} against 9.3–9.4 cm^{-1}, and the bands near 164, 194 and 314 cm^{-1} show the largest broadening. The 678 and 709 cm^{-1} bands are weak and diffuse. In addition, the sol–gel spectrum has a strong sloping background (about 8000–17000 counts, roughly ten times that of the solid-state samples) and a weak band near 926 cm^{-1}. Together these features indicate somewhat lower structural order in the sol–gel sample, for example finer crystallites or more defects. The higher laser power may also contribute to the shift and broadening. The main modes remain sharp, so the effect is modest. As shown in Figure 2 (a) Shift of the Raman band positions: Eu^{3+}-doped solid-state samples (mean of 1% and 2%) relative to ZWO-SS, and ZWO-SG relative to the doped samples. (b) Fitted FWHM of selected bands for the four samples.

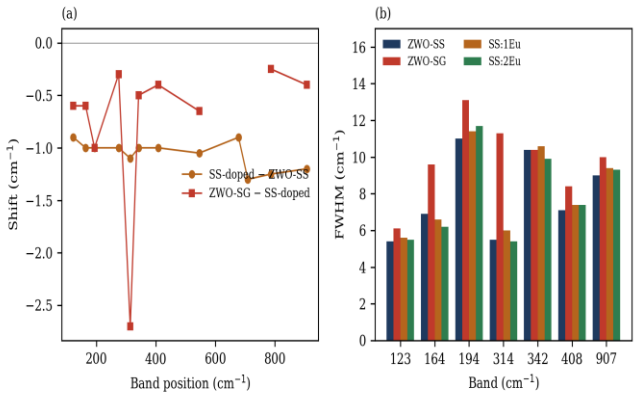


Figure 2 (a) Shift of the Raman band positions: Eu^{3+}-doped solid-state samples (mean of 1% and 2%) relative to ZWO-SS, and ZWO-SG relative to the doped samples. (b) Fitted FWHM of selected bands for the four samples

Conclusion

Raman spectroscopy was used to study pure $ZnWO_4$ prepared by solid-state and sol–gel methods and solid-state $ZnWO_4$ doped with 1% and 2% Eu^{3+}. All samples exhibited the complete set of vibrational modes of monoclinic wolframite, dominated by the symmetric W–O stretching band near 907 cm^{-1}, so both synthesis routes give the wolframite structure, which is retained on doping. The 1% and 2% Eu^{3+} samples gave practically identical spectra, with no new bands and no measurable change in band position or width, so no Eu^{3+}-dependent modification of the WO_6 framework was detected in this range. The uniform downshift of about 1 cm^{-1} of all bands relative to the pure solid-state sample reflects the different excitation and grating, not doping. The sol–gel sample showed slightly lower band positions, broader low-frequency bands, a strong fluorescent background and a weak band near 926 cm^{-1}, indicating somewhat lower structural order. Measuring the pure solid-state sample under the doped-sample conditions and repeating the sol–gel scan are recommended.

International Research Journal on Advanced Engineering and Management
https://goldncloudpublications.com
https://doi.org/10.47392/IRJAEM.2026.0410
e ISSN: 2584-2854
Volume: 04 Issue: 10
October 2026
Page No: 2910 - 2916

References

[1]. N. B. A. Duong, N. Van Du, N. V. Duong, T. T. H. Tam, L. T. Ha, and N. D. Hung, " Optimization and Evaluation of Eu^{3+} - Doped Zinc Molybdate Phosphors for Red Emission Performance in LED Devices ," J. Phys. Conf. Ser., vol. 3284, no. 1, p. 012066, 2026, doi: 10.1088/1742-6596/3284/1/012066.

[2]. Q. Ning, C. Zhou, and Y. Shi, "The influence of Eu^{3+} doping on the studies of luminescent properties and quantum efficiency of $ZnWO_4$ phosphor," J. Mater. Sci. Mater. Electron., vol. 31, no. 13, pp. 10499–10511, 2020, doi: 10.1007/s10854-020-03598-y.

[3]. 3] F. Zunia, M. Raeisi, S. Alamdari, and N. H. Dehkordi, "Synthesis and Structural Investigation of Erbium-Doped $ZnWO_4$ Nanocrystals," Nanochemistry Res., vol. 9, no. 1, pp. 28–34, 2024, doi: 10.22036/NCR.2024.01.04.

[4]. G. Li, G. Cai, and X. Wang, "Local Structure–Luminescence Correlation in Eu^{3+} -Doped Phosphors: A Comprehensive Review," Adv. Photonics Res., vol. 6, 2025, doi: 10.1002/adpr.202500142.

[5]. Y. Wang, A. Liu, Z. Li, Z. Wang, and Y. Chen, "Preparation and properties of Eu^{3+} doped tungstate red phosphor powders," Process. Appl. Ceram., vol. 18, pp. 156–161, Jun. 2024, doi: 10.2298/PAC2402156W.

[6]. Vinod Kumar and Rakesh Kumar, "State-of-the-Art Developments in Luminescent Nanophosphors for Solid-State Technologies," Int. J. Innov. Sci. Eng. Manag., vol. 5, no. 3, pp. 363–383, 2026, doi: 10.69968/ijisem.2026v5i3363-383.

[7]. Rituparna Chatterjee, G. C. Das, and K. K. Chattopadhyay, "Luminescence properties of nano and bulk $ZnWO_4$: Eu^{3+} phosphors for solid state lighting applications," Mater. Res. Express, 2020.

[8]. H. Zou and X. Wang, "Preparation and luminescence properties of $ZnWO_4$: Eu^{3+},Tb^{3+} phosphors," Luminescence, vol. 36, pp. 1452–1458, Jun. 2021, doi: 10.1002/bio.4086.

[9]. Q. Ning, C. Zhou, and Y. Shi, "Effect of Eu^{3+} doping on $ZnWO_4$ phosphors luminescent properties and study of J-O theory," J. Solid State Chem., vol. 290, p. 121458, Jul. 2020, doi: 10.1016/j.jssc.2020.121458.

[10]. H. L. Abubakar, J. O. Tijani, S. A. Abdulkareem, A. Mann, and S. Mustapha, "A review on the applications of zinc tungstate ($ZnWO_4$) photocatalyst for wastewater treatment," Heliyon, vol. 8, no. 7, p. e09964, 2022, doi: 10.1016/j.heliyon.2022.e09964.

[11]. A. M. Abdelraheem et al., "High-performance zinc tungstate photocatalyst: tailoring crystallinity, bandgap, and charge separation via controlled calcination," Sci. Rep., vol. 16, no. 27432, pp. 1–19, 2026, doi: 10.1038/s41598-026-64862-5.

[12]. L. X. Lovisa, J. V. T. Pedron, T. B. O. Nunes, C. R. S. de Oliveira, M. R. da Rocha, and M. Siu, "Investigation of the influence of Eu^{3+} doping on ZnO: impact on microstructural and optical properties," Appl. Phys. A Mater. Sci. Process., vol. 132, no. 687, 2026, doi: 10.1007/s00339-026-09884-6.

[13]. S. Tahir and B. Want, "Doping effect of Europium (Eu) on flower-like ZnO nanostructures: shape variations, optical properties and its applicability in electrochemical sensing of heavy metal (Lead) ion detection," Appl. Phys. A, vol. 130, Mar. 2024, doi: 10.1007/s00339-024-07358-1.

[14]. F. T. Geldasa, H. F. Etefa, and F. B. Dejene, "Effect of Europium Doping on the Structural, Morphological, and Luminescent Properties of $Y_3Al_5O_{12}$ Phosphors Produced by Combustion Method," J. Fluoresc., vol. 35, pp. 10423–10430, 2025, doi: 10.1007/s10895-025-04319-6.

International Research Journal on Advanced Engineering and Management
https://goldncloudpublications.com
https://doi.org/10.47392/IRJAEM.2026.0410
e ISSN: 2584-2854
Volume: 04 Issue: 10
October 2026
Page No: 2910 - 2916

[15]. H. Syiemlieh, J. Saji, O. Manners, and V. Dubey, "Effect of europium concentration on the thermoluminescence and photoluminescence properties of $CaSO_4:Eu^{3+}$ phosphors for dosimetry and display applications," Next Mater., vol. 13, no. July, p. 102819, 2026, doi: 10.1016/j.nxmate.2026.102819.

[16]. R. N. Prajapati, A. P. Mishra, Y. R. Parauha, and S. J. Dhoble, "Self-luminescence properties of $Zn_3(VO_4)_2$ phosphors and the effect of Eu3+ ions doping," Bull. Mater. Sci., vol. 47, no. 172, 2024, doi: 10.1007/s12034-024-03263-8.

[17]. K. Subbotin et al., "Influence of Accidental Impurities on the Spectroscopic and Luminescent Properties of ZnWO4 Crystal," Materials (Basel)., vol. 16, no. 2611, pp. 1–17, 2023.

[18]. T. N. L. Tran, A. Chiasera, A. Lukowiak, and M. Ferrari, "Eu^{3+} as a Powerful Structural and Spectroscopic Tool for Glass Photonics," Materials (Basel)., vol. 15, no. 1847, pp. 1–11, 2022, doi: 10.3390/ma15051847.

[19]. K. V Dabre and S. J. Dhoble, "Photoluminescence properties of $ZnWO_4:Dy^{3+}$ phosphor," Recent Res. Sci. Technol., vol. 4, no. 8, pp. 102–103, 2012.